IOP Conference Series:
Earth and
Environmental Science

PAPER • **OPEN ACCESS**

Improving a DSM Obtained by Unmanned Aerial Vehicles for Flood Modelling

To cite this article: Sandra Mourato *et al* 2017 *IOP Conf. Ser.: Earth Environ. Sci.* **95** 022014

IOP Conf. Series: Earth and Environmental Science **95** (2017) 022014 doi:10.1088/1755-1315/95/2/022014

Improving a DSM Obtained by Unmanned Aerial Vehicles for Flood Modelling

Sandra Mourato [1,5], Paulo Fernandez [2,5], Luísa Pereira [3,6], Madalena Moreira [4,5]

[1] School of Technology and Management, Polytechnic Institute of Leiria. Morro do Lena - Alto do Vieiro, Apartado 4163, 2411-901 Leiria, Portugal

[2] Polytechnic Institute of Castelo Branco. Quinta da Senhora de Mércules, Apartado 119, 6001-909 Castelo Branco, Portugal

[3] ESTGA, Universidade de Aveiro. Rua Comandante Pinho e Freitas, nº 28. 3750 - 127 Águeda, Portugal

[4] Universidade de Évora - Escola de Ciências e Tecnologia. Pólo da Mitra, 7006-554 Évora, Portugal

[5] ICAAM - Instituto de Ciências Agrárias e Ambientais Mediterrânicas, Universidade de Évora, 7006-554 Évora, Portugal

[6] Centro de Investigação em Ciências Geo-Espaciais, Universidade do Porto, Porto, Portugal

sandra.mourato@ipleiria.pt

Abstract. According to the EU flood risks directive, flood hazard map must be used to assess the flood risk. These maps can be developed with hydraulic modelling tools using a Digital Surface Runoff Model (DSRM). During the last decade, important evolutions of the spatial data processing has been developed which will certainly improve the hydraulic models results. Currently, images acquired with Red/Green/Blue (RGB) camera transported by Unmanned Aerial Vehicles (UAV) are seen as a good alternative data sources to represent the terrain surface with a high level of resolution and precision. The question is if the digital surface model obtain with this data is adequate enough for a good representation of the hydraulics flood characteristics. For this purpose, the hydraulic model HEC-RAS was run with 4 different DSRM for an 8.5 km reach of the Lis River in Portugal. The computational performance of the 4 modelling implementations is evaluated. Two hydrometric stations water level records were used as boundary conditions of the hydraulic model. The records from a third hydrometric station were used to validate the optimal DSRM. The HEC-RAS results had the best performance during the validation step were the ones where the DSRM with integration of the two altimetry data sources.

1. Introduction

Hydraulic models are essential tools for flood hazard prediction. These models need to be calibrated and validated, so monitoring the water levels flood events is important to improve flood hazard mapping. The representation of the terrain surface is another critical factor in the hydraulic flood modelling because it affects the flood hydrogram and the flood extent [1]. The spatial (horizontal and vertical)

resolution and the geometric accuracy of the topographic data may impact on the results of hydraulic flood modelling producing large differences [2-3]. The topographic data also affect the computational domain in a hydraulic simulation and represent the surface terrain in the model through elevations defined along cross-sections (1D model) or mesh nodes (2D model) [4-6]. The accuracy of the modelled terrain surface is affected by several factors such as the precision and the density and distribution of the measured elevation points, the interpolation algorithm and the spatial resolution of the profiles or of the meshes [7-9].

The roughness coefficients are a parameter of the hydraulic model, which, when correctly defined, allows one to obtain a distribution of the velocity and the shear stress very close to the reality, and a good prediction of free surface flow. Because they result from the combination of runoff surface characteristics that are influenced by several flow characteristics, such as water depth and velocity, roughness coefficients are a very important input data for the flood hydraulic modelling [10-12]. A land use map produced with high resolution aerial images can be used to represent the spatial distribution of the roughness coefficients in the flooded areas [11, 13].

Promising results in improving flood model performance have been obtained using the integration of LiDAR (Light Detection and Ranging) data [14-15] with digital cartography and orthoimages [3, 16]. Currently, images acquired with Unmanned Aerial Vehicles (UAV) are seen as a good alternative data sources to obtain spatial data that represent the terrain surface with a high level of detail [15, 17]. The UAV offers a fast and accurate way to acquire aerial images at a relatively low cost with resolution and accuracy typically in the range of a few centimetres [15, 17]. Compared to traditional airborne remote sensing, the UAV enable rapid operation to obtain high frequency multi-temporal and high resolution images [15].

This study aims to address the hydraulic modelling and uncertainties in the spatial data that may affect the flood hazard mapping. The objective of this study is to produce an optimal Digital Surface Runoff Model (DSRM), for input in a hydraulic flood model, by using an improved Digital Surface Model (DSM) produced with UAV´s images and GPS data. Hydraulic computations were made with the HEC-RAS, a model that can simulate both steady and unsteady state flow conditions.

The paper outline is as follows: Section 1 introduces the background and the aim of the study. Section 2 presents the study area, and describes the different DSRM creation and the flood modelling approach. The results are presented and discussed in Section 3 and finally some conclusions are presented in Section 4.

2. Materials and methods

2.1. Study site and data

The hydraulic modelling was carried out on an 8.5 km extent of the Lis river near Monte Real, situated in the river basin district of *Vouga*, *Mondego* and *Lis* (Centre of Portugal), where flooding occurs (Figure 1).

Three types of basic data were collect to produce the DSRM: aerial images, the X, Y and Z coordinates of points along river cross-sections and water level at three hydrometric stations. To acquire the aerial images, two flights were performed on August 2015, at a height of approximately 170 m using the eBee UAV from Sensefly (*www.sensefly.com/drones/ebee.html*). The weather conditions were good with the sky slightly cloudy. The eBee can cover up to 12 km^2 in a single automated flight, while flights over smaller areas, flown at lower altitudes, can acquire images with a spatial resolution of 2.3 cm. The eBee sets the flight planning and management through eMotion software. It was used a flight plan with a forward and side overlap of 60%. The eBee uses a radio link to communicate with eMotion. A Canon PowerShot ELPH 110 HS camera has been installed on the UAV and collected 3680 images in total. This camera allows capturing RGB images with a resolution of 16.1 MP (approximately 4608x3456 active pixels). The eBee's flight optimization was produced by the analyses of data from an inertial measurement unit and onboard GPS.

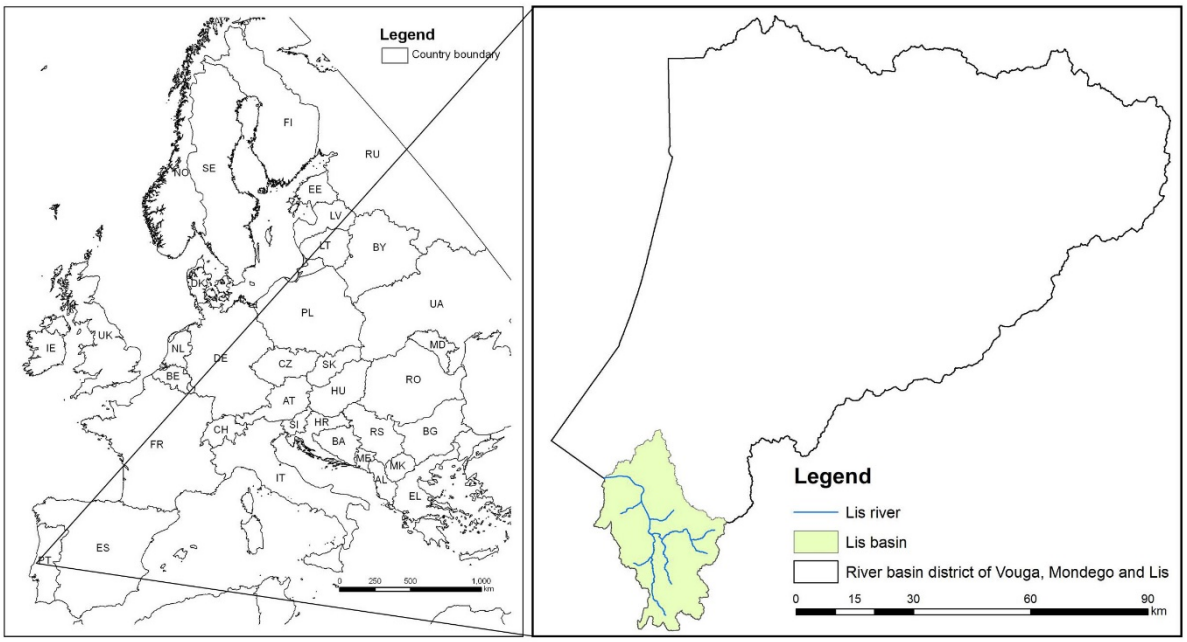

Figure 1. Study site location

The area covered by the flights is 18 km^2 and there were 19 Ground Control Points (GCPs) well distributed within the surveyed area. The positions of the GCP were measured immediately prior to the imaging to ensure coincidence of positioning and imaging. High-precision GPS system (Topcon HiPER Lite) with RTK (Real Time Kinematic) corrections was used with an expected horizontal and vertical accuracy of, respectively 1 cm and 1.5 cm. The coordinate system used were the Portuguese Projection Cartographic System PT-TM06/ETRS89 for the planimetry and the *Cascais* Datum for the altimetry.

The images were processed and analysed using the dedicated image processing software Pix4Dmapper Pro, developed at Computer Vision Lab in Switzerland (http://pix4d.com). The Pix4Dmapper Pro can be applied for converting thousands of images, taken by lightweight UAV into geo-referenced point clouds, 2D or 3D surface models and orthomosaics. The image processing performs a bundle block adjustment, including a camera calibration for determining the parameters of the inner orientation, i.e., the focal length, and the image coordinates of the principal point. Values for the lens distortion are also computed. The calibrated values of the inner orientation are tabulated in Table 1.

In the pipeline of the process, after the bundle block adjustment that gives the exterior orientation parameters of the images, a point cloud was produced based of the matching algorithm SIFT [18]. The DSM was then created by means the height values of the points in the cloud, with a pixel of 5 cm using the inverse distance weight interpolation method. The DSM was further used with the images to produce an orthomosaic. Both, the DSM and the orthomosaic were exported as GeoTIFF.

Table 1. Inner orientation parameters.

	Focal length	Principal point x	Principal point y
Calibrated values	4.402 mm	3.169 mm	2.387 mm

The ground survey to obtain the river cross-sections was carried out also in August 2015 using the GPS device utilized for the acquisition of the GCP. The ground survey based on GPS has the advantage of obtaining high precision topographic data (1-1.5 cm) and, unlike the photogrammetric survey, is able

to capture channel bed features underneath the water and vegetation. During this time of the year, the water depths of Lis river are usually low (i.e. not exceeding 0.5 m). A total of 42 cross-sections were surveyed with a spacing of, approximately 200 m (Figure 2).

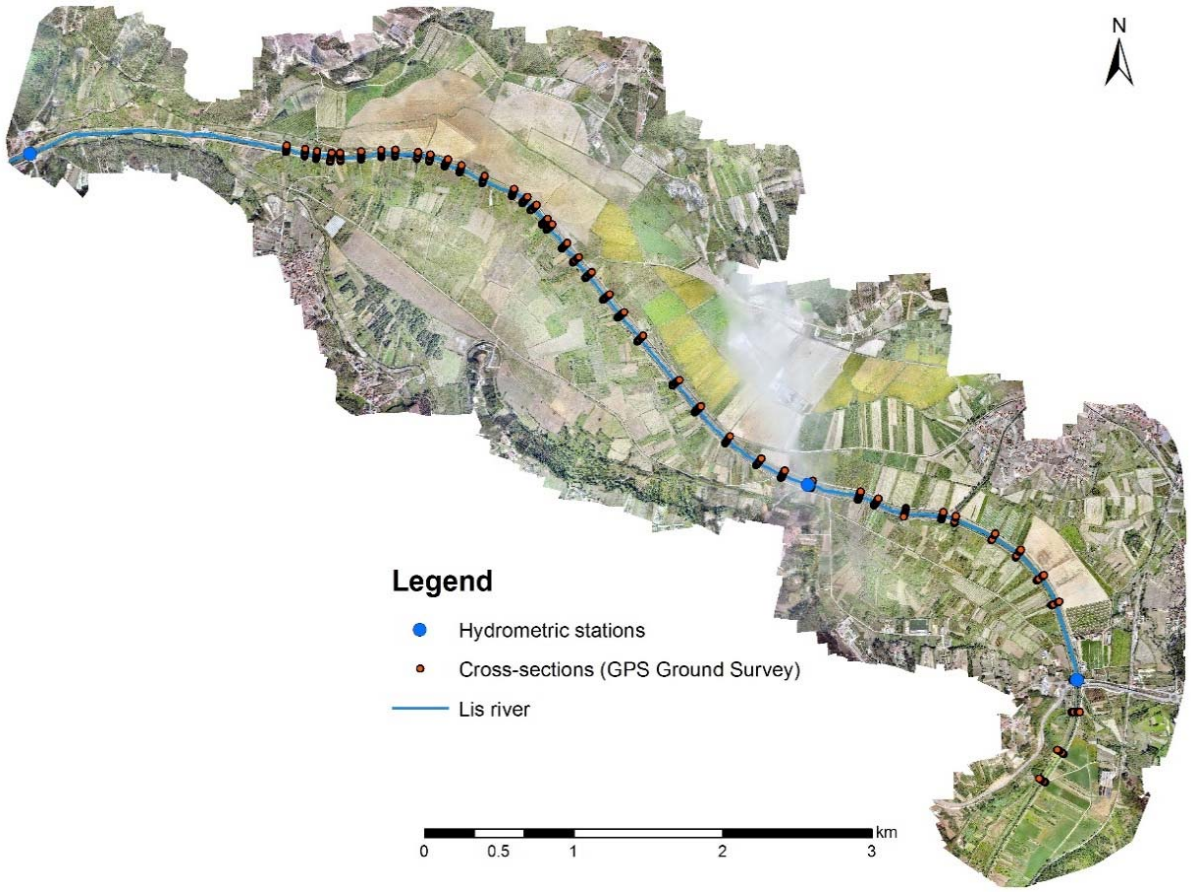

Figure 2. Cross-sections GPS ground survey and hydrometric sections

In order to calibrate and validate the hydraulic model, the water depth was measured at three hydrometric stations (Figure 2). Two recorded stage hydrographs were used as boundary conditions (*Monte Real e Ponte da Bajanca*) and a third recorded stage hydrograph (*Ponte da Carreira*) was used for the hydraulic model validation. The National Water Service (*www.snirh.pt*) provides hourly data for the Monte Real station whereas the data from the other two hydrometric stations were obtained at a 15 minutes' interval. This paper addresses a flood event that occurred between 1/Feb/2016 and 18/Feb/2016. The water level records on the *Monte Real* and the *Ponte da Bajanca* stations are illustrated in Figure 3. The records at *Ponte da Bajanca*, located 3 km from the Lis river mouth, are important because they reflect the tidal effect.

2.2. DSM and DTM

For this study three different altimetry data sources were used: (1) a Digital Terrain Model (DTM), (2) a Digital Surface Model (DSM), and (3) a GPS ground survey.

A DSM contains, in addition to the elevation values of the bare ground, those of the objects on it like buildings, trees and other vegetation. A Digital Terrain Model (DTM) represents the terrain surface and is obtained from the DSM by removing, or filtering, those objects. Subtraction of the DTM from the DSM gives the normalised Digital Surface Model (nDSM), i.e. a model that contains the height values

of the objects. The purpose of the DSRM production is the coherent representation of terrain model for flood modelling.

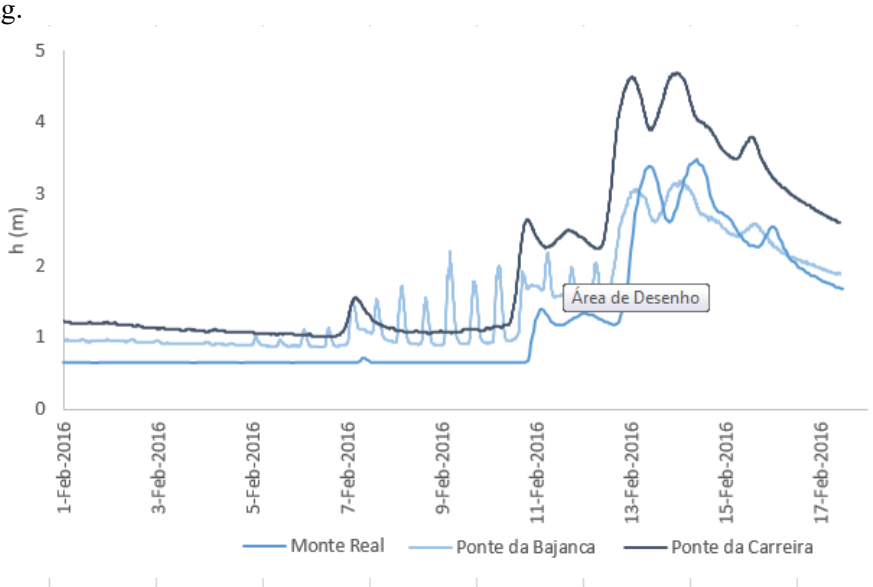

Figure 3. Water levels at *Monte Real*, *Ponte Carreira* and *Ponte da Bajanca* stations

The optimal Digital Surface Runoff Model (DSRM) was selected amongst four DSRM: 1) DSRM1, produced with the DSM in raster format, 2) DSRM2, a raster made with the DTM and the nDSM (only the pixels with height values less than 2 m), 3) DSRM3, the same as DSRM1 but integrated with the GPS data, and 4) DSRM3, the same as DSRM2 but integrated with the GPS data. A map of Manning's n roughness coefficients for the channel and floodplain was produced from the orthoimage and field survey.

2.3. Hydraulic modelling

Hydraulic computations were made with the HEC-RAS 5.0.1 developed by the Hydrologic Engineering Center (HEC) of the United States Army Corps of Engineers Hydrologic Engineering Center [19]. The HEC-RAS system contains the following river analysis components: (1) steady flow water surface profile computations; (2) one-dimensional and/or two-dimensional unsteady flow simulation. Data requirements for HEC-RAS include topographic information in the form of a series of cross-sections, roughness coefficients in the form of Manning's n values across each cross-section, and flow data including flow rates, water depth, and boundary conditions. The HEC-GeoRAS extension was used to create geometric input data that was imported into the HEC-RAS.

The definition of the cross-sections is determined by the resolution of the topographic data source. A map showing the Manning's n roughness coefficients for the different channel and floodplain elements was produced from the orthoimage of the area and field survey establishing the values presented in Table 2 [11, 13, 20-21].

Cross-sections are a very important input data and they were defined in the way they best characterize the terrain. Therefore, they were created in places with changing flow direction because the model tends to linearize segments between the cross-section profiles. Model instability can be caused by cross-sections´ spacing too wide or too narrow. When cross-sections are too far apart, numerical diffusion can become an issue, while cross-sections too nearby can result in over-steepened flood waves. Equation 1 was used to calculate the cross-sections spacing [22] where *D* is the average bankfull depth of the channel in m, and S is the average bed slope.

$$\Delta X = 0.15 \times D/S \quad (1)$$

Table 2. Manning roughness coefficients used for each land use class.

Land use classes	Manning roughness coefficient
Discontinuous urban fabric	0.120
Industrial units	0.085
Annual crops associated with permanent crops	0.038
Complex cultivation patterns	0.040
Vineyards	0.038
Natural grassland	0.035
Broad-leaved forest	0.160
Coniferous forest	0.170
Mixed forest	0.165
Heathland	0.070
Sclerophyllous vegetation	0.035

The channel bed slope is 0.0021m/m. Considering a medium depth of 3.5 m, the maximum cross-section´ spacing is 250 m. In Hec-RAS, a total of 47 cross-sections were created along the Lis river extent with an average separation distance of 180 m (Figure 4).

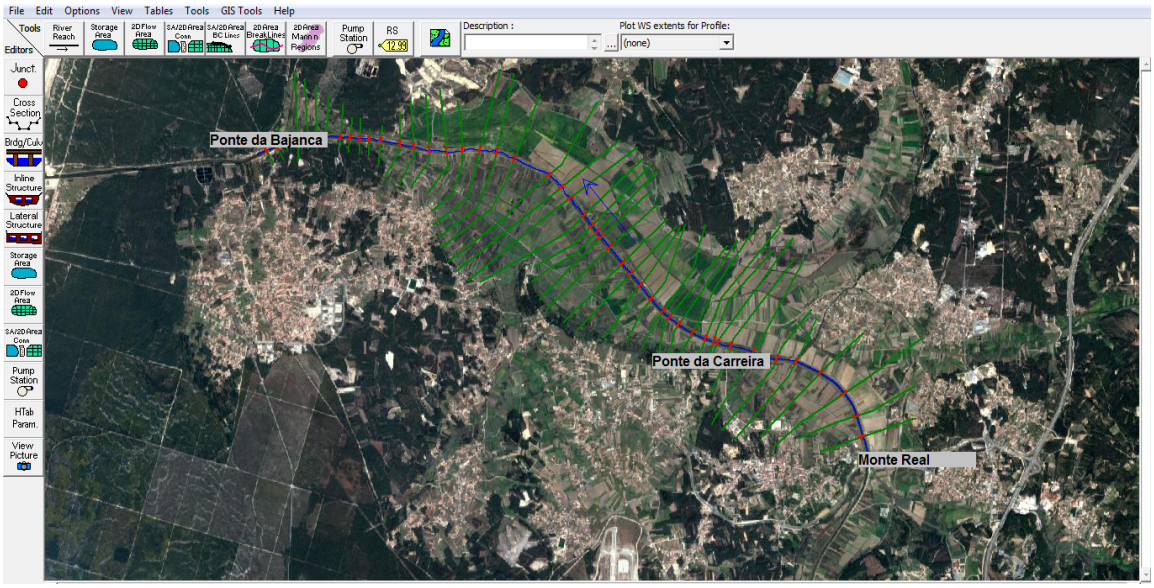

Figure 4. River (blue line), bank stations (red dots), cross sections (green lines) used in the hydraulic model

Four hydraulic simulations were performed. For each simulation, the lay-out of the 47 cross-sections and the Manning's n roughness coefficients map are maintained whereas the height values of the points along the cross-sections are interpolated from each of four produced DSRM. The simulated water levels, for each simulation, were compared with the records at *Ponte da Carreira* hydrometric station.

3. Results and discussion

Figure 5 compares the simulated results with the recorded water levels at *Ponte da Carreira*. It is found that the hydraulic simulations done with the DSRM1 and DSRM2 do not agree with the water level records. The hydraulic model has presented several numerical instabilities, mainly due to the fact that the bed river slope has a very irregular longitudinal profile in which significant sudden river bed levels rises occur.

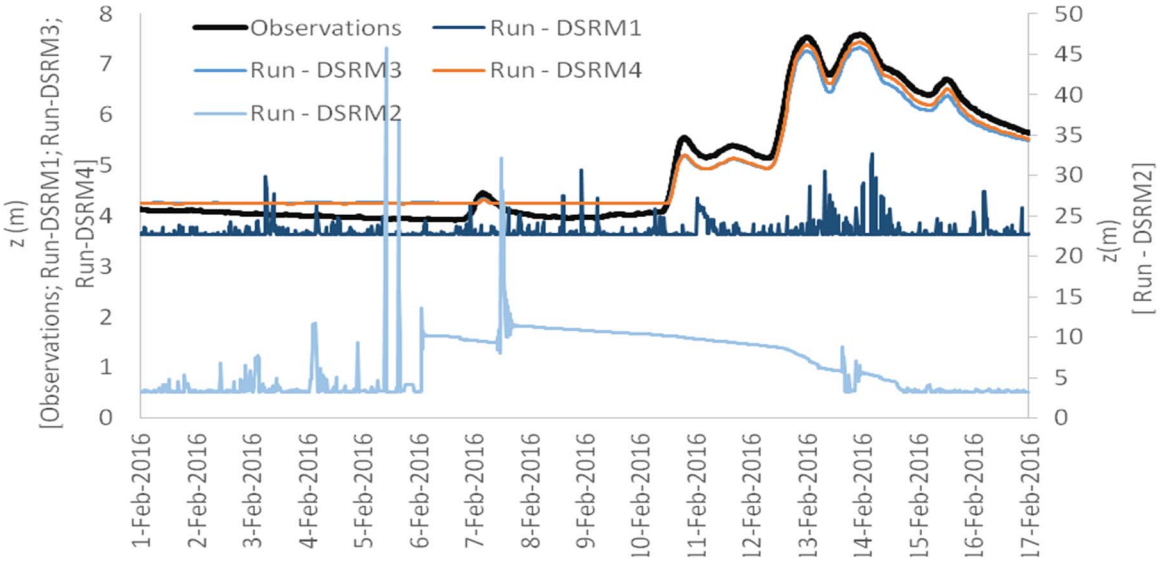

Figure 5. Simulated and recorded water levels at *Ponte da Carreira* station.

Figure 6 presents the river bed longitudinal profile for each one of the four DSRM. In order to be able to use these DSRM it would be necessary to model the river bed to eliminate those sudden elevation changes.

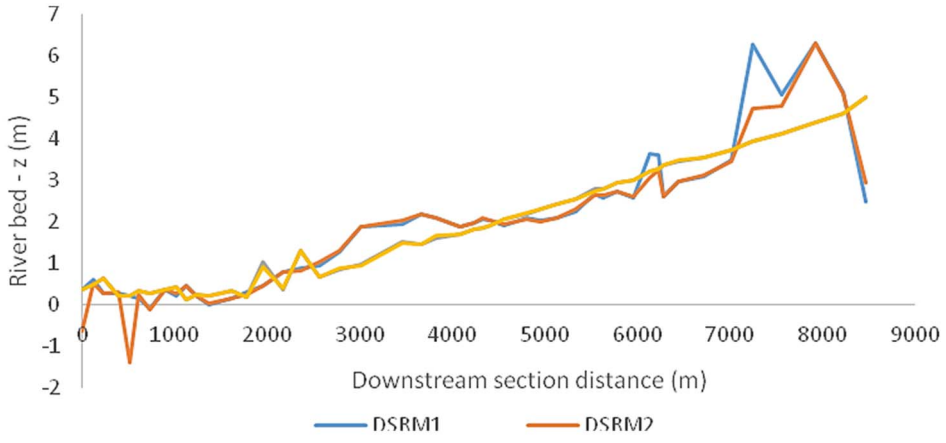

Figure 6. River bed longitudinal profile for the four DSRM

On the other hand, when the hydraulic simulations were done with the DSRM3 and with the DSRM4, the sudden variations in the river bed are no longer observed, and the model does not have numerical instabilities. The results were very similar for both DSRM with correlations as high as 99.30% and 99.26% respectively. After the peak in the descending branch, the water levels produced by using the DSRM4 have more similarities with the records.

4. Conclusions

Four different DSRM were produced with DSM or with the DTM obtained from the DSM by filtering the objects integrated with the objects with height less than 2 m, respectively. The hydraulic modelling results obtained with the DSRM1 and DSRM2 have presented several numerical instabilities even with the Samuel's Equation for Cross Section Spacing verification.

The integration of the DSRM1 and DSRM2 with the channel bed features obtained with cross-sections carried out with a high precision GPS system resulted in the DSRM3 and DSRM4, respectively. The hydraulic modelling with the DSRM3 and DSRM4 allowed a correlation with the measured hydrograph as high as 99.30% and 99.26% respectively.

According with these results, and for the topographic characteristics and land cover of the study area, it is not justified the filtering effort. The integration of GPS cross-section data with the DSM as obtained directly from the photogrammetric point cloud appears sufficient. Regarding the results, the including the objects with heights less than 2 m and including the GPS information may be more suitable for high rate flows. Nonetheless, future work should validate the flood extent by using both DSRM3 and DSRM4.

The optimization of the DSRM is the result of the integration of the GPS data that model the river bed. Therefore, bathymetric data is of paramount importance. The efforts on the collection of height data, both from the terrain surface and river bed, using different techniques, such as photogrammetry, GPS and bathymetry, and consequently different equipment and software, may be replaced by the new developments in LiDAR technology. In fact, a multispectral (or with a green channel) airborne LiDAR sensor, mounted in an aircraft or UAV, permits the collection of points both from the terrain surface and the river bed at the same acquisition. Furthermore, unlike DRSM produced by using LiDAR, those created with images of highly vegetated areas as those along the river banks, are inaccurate for the vegetation cannot be entirely filtered out.

Acknowledgments
The data of this work is funded by POCTEP - European Regional Development Fund under the project Territorial and Environmental Observatory of the Cross-border Region composed by Alentejo and Centro Regions of Portugal and Extremadura Region of Spain (OTALEX-C). This work is funded by National Fund through FCT – Foundation for Science and Technology under the Project UID/AGR/00115/2013.

References

[1] M. S. Horritt, and P. D. Bates, "Effects of spatial resolution on a raster based model of flood flow ", *Journal of Hydrology*, vol. 253, pp. 239-49 2001.
[2] A. Casas, G. Benito, V. R. Thorndycraft, and M. Rico, "The topographic data source of digital terrain models as a key element in the accuracy of hydraulic flood modelling", *Earth Surface Processes and Landforms*, vol. 31, pp. 444-56 2006.
[3] P. Fernandez, Urban flood risk assessment by integrating LiDAR data and large scale cartography: University of Évora; 2015.
[4] M. Podhorányi, J. Unucka, P. Bobál, and V. Říhová, "Effects of LIDAR DEM resolution in hydrodynamic modelling: model sensitivity for cross-sections", *International Journal of Digital Earth*, vol. 6, pp. 3-27, 2013.
[5] A. Cook, and V. Merwade, "Effect of topographic data, geometric configuration and modeling approach on flood inundation mapping", *Journal of Hydrology*, vol. 377, pp. 131-42, 2009.
[6] N. M. Hunter, P. D. Bates, S. Neelz, G. Pender, I. Villanueva, N. G. Wright, D. Liang, R. A. Falconer, B. Lin, S. Waller, A. J. Crossley, and D. C. Mason, "Benchmarking 2D hydraulic models for urban flooding", *Water Management* vol. 161, pp. 13-30, 2008.
[7] F. J. Aguilar, F. Agüera, M. A. Agullar, and F. Carvajal, "Effects of terrain morphology, sampling density, and interpolation methods on grid DEM accuracy", *Photogrammetric Engineering and Remote Sensing*, vol. 71 (7), pp. 805-16 2005.
[8] V. Chaplot, F. Darboux, H. Bourennane, S. Leguédois, N. Silvera, and K. Phachomphon, "Accuracy of interpolation techniques for the derivation of digital elevation models in relation to landform types and data density", *Geomorphology*, vol. 77, pp. 126-41, 2006.
[9] P. F. Fisher, and N. J. Tate, "Causes and consequences of error in digital elevation models", *Progress in Physical Geography*, vol. 30, pp. 467-89, 2006.

[10] A. De Roo, J. Van Der Knijff, G. Schmuck, and P. Bates, "A simple floodplain inundation model to assist in floodplain management", *New Trends in Water and Environmental Engineering for Safety and Life: Eco-compatible Solutions for Aquatic Environments'*, 2000.
[11] M. D. Wilson, and P. M. Atkinson, "The use of remotely sensed land cover to derive floodplain friction coefficients for flood inundation modelling", *Hydrological Processes*, vol. 21, pp. 3576-86, 2007.
[12] M. S. Horritt, and P. D. Bates, "Evaluation of 1D and 2D numerical models for predicting river flood inundation", *Journal of Hydrology* vol. 268, pp. 87-99, 2002.
[13] J. E. Schubert, B. F. Sanders, M. J. Smith, and N. G. Wright, "Unstructured mesh generation and landcover-based resistance for hydrodynamic modeling of urban flooding", *Advances in Water Resources*, vol. 31, pp. 1603-21, 2008.
[14] P. D. Bates, K. J. Marks, and M. S. Horritt, "Optimal use of high-resolution topographic data in flood inundation models", *Hydrological Processes*, vol. 17, pp. 537-57, 2003.
[15] C. Flener, M. Vaaja, A. Jaakkola, A. Krooks, H. Kaartinen, A. Kukko, E. Kasvi, H. Hyyppä, J. Hyyppä, and P. Alho, "Seamless Mapping of River Channels at High Resolution Using Mobile LiDAR and UAV-Photography", *Remote Sensing*, vol. 5, 2013.
[16] D. C. Mason, M. S. Horritt, N. M. Hunter, and P. D. Bates, "Use of fused airborne scanning laser altimetry and digital map data for urban flood modelling", *Hydrological Processes*, vol. 21, pp. 1436-47, 2007.
[17] L. Pádua, J. Vanko, J. Hruška, T. Adão, J. J. Sousa, E. Peres, and R. Morais, "UAS, sensors, and data processing in agroforestry: a review towards practical applications", *International Journal of Remote Sensing*, vol. 38, pp. 2349-91, 2017.
[18] D. G. Lowe, "Object Recognition from Local Scale-Invariant Features", *Proceedings of the International Conference on Computer Vision*, vol. 2, pp. 1150, 1999.
[19] U.S. Army Corps of Engineers, Hydrologic Engineering Center, HEC-RAS River Analysis System, User's Manual, Version 5.0. Hydrologic Engineering Center, Davis, CA., 2016.
[20] V. T. Chow, Open-Channel Hydraulics. McGraw-Hill Inc, 1988.
[21] C. J. Van der Sande, S. M. De Jong, and A. P. J. De Roo, "A segmentation and classification approach of IKONOS-2 imagery for land cover mapping to assist flood risk and flood damage assessment", *International Journal of Applied Earth Observation and Geoinformation*, vol. 4, pp. 217-29, 2003.
[22] P. G. Samuels, "Backwater Lengths in Rivers", *Proceedings of the Institution of Civil Engineers*, vol. 87, pp. 571-82, 1989.